Adaptive Modulation and Feedback Strategy for an Underwater Acoustic Link

Wu Shuangshuang
Department of Electrical and Computer Engineering, National University of Singapore

Prasad Anjangi
Subnero Pte. Ltd. Singapore

Mandar Chitre
Department of Electrical and Computer Engineering & ARL, Tropical Marine Science Institute, National University of Singapore

***Abstract*—As underwater acoustic channels are highly variable, both temporally and spatially, it is impossible to design a single communication scheme that works well everywhere and at all times. Adaptive modulation and coding (AMC) techniques can help determine the best communication scheme to use for a particular channel, but require an accurate model to predict communication performance. We propose a bit error rate (BER) estimation model that fuses domain knowledge with experimental data, yielding BER estimates that are consistent with experimental observations. Predictions from such a model are used to drive an AMC algorithm to maximize communication throughput. For AMC, regular feedback from the receiver to the transmitter is necessary to gather channel state information (CSI). On the one hand, obtaining feedback too often drastically impacts the communication throughput in channels with long propagation delays, but on the other hand, insufficient feedback leads to poor AMC decisions and hence poor throughput. We propose a dynamic feedback strategy to automatically find the right balance and maximize communication performance.**

I. Introduction

Given the spatial and temporal variability in underwater acoustic channels, a single communication scheme that performs well in all channels at all times is impossible to find. Adaptive modulation and coding (AMC) techniques can help alleviate this problem by finding the best communication scheme to use for reliability and high throughput [1]–[5].

Channel state information (CSI) gathered through the feedback packets assists in predicting the channel at least one travel time ahead. This allows for the selection of physical-layer parameters, in turn enabling adaptive strategies [6], [7]. BER is a common figure of merit for evaluating the performance of a digital communication system, and Monte Carlo (MC) error count is regarded as a robust BER estimation strategy [8], [9]. The MC strategy, however, always requires a significant accumulation of transmission samples to facilitate Bayesian model fusion with a Bernoulli distribution to estimate BER [10], [11]. When an AMC algorithm changes communication schemes often, MC techniques perform poorly due to scarcity of transmission samples of each scheme. The authors in [12] theoretically predict BER as a function of signal-to-noise ration (SNR) based on various channel models (Rayleigh, Rician, and Nakagami). Some studies introduced machine learning (ML) algorithms to estimate median BER as a function of SNR [13] and channel-physics-related parameters (e.g., delay spread, Doppler spread etc.) [14]. It is recognized that channel physics information such as delay spread, Doppler spread, and ambient noise level can provide a basis for evaluating the average channel performance of various AMC schemes (e.g. packet success probability [15]).

There is also an inherent trade-off between CSI feedback periodicity from the receiver and the estimated channel's accuracy. Due to the long propagation delays incurred in underwater acoustic communication, it is expensive to collect CSI information for every packet that is transmitted [16], [17]. In [18]–[20], the temporal correlation in the channel is exploited for decision making for the waiting interval between consecutive feedback for short-range wireless communication. Considering a more general case, the authors in [21] use an ML-based feedback scheme that dynamically changes the CSI feedback interval, but ignores propagation delays.

In this paper, we build on the work presented in [15], [22] to formulate a channel-physics-driven BER estimation model for AMC, and validate it using the experimental data collected in Singapore waters. Since the model can be utilized to infer BER of any communication scheme without the need to transmit, we can significantly reduce the number of transmissions required in converging to the optimal scheme. We also design an adaptive feedback strategy to determine the number of transmission packets before the receiver sends back the feedback information. Such feedback strategy aids in achieving better AMC performance by reducing the overhead due to the the large propagation delays.

II. Problem formulation

Information packets are transmitted from a transmitter (Tx) to a receiver (Rx) deployed at a distance l from the Tx. This point-to-point channel is modeled as a Binary Symmetric Channel (BSC) [23]. Prior to each packet transmission, we select a communication scheme $\boldsymbol{a} \in \mathcal{A}$ to suit the current channel conditions, based on the best estimate of the channel that we have. We also decide on a feedback report interval (FRI), i.e., the number of transmission packets $h \in \mathcal{H}$ between two consecutive feedback packets. The feedback is sent over a robust link for providing CSI. Therefore the decision space (also known as the *action space*) has a cardinality $|\mathcal{A} \times \mathcal{H}|$. An *agent* learns a policy Π via continuous interaction with the environment to make sequential decisions on $\boldsymbol{a}$ and h to transmit totally N bits. The policy Π is a function that maps from the state space to the action space, i.e., $\Pi : \mathcal{S} \rightarrow [\mathcal{A} \times \mathcal{H}]$. After transmitting the j^{th} packet, the agent is in state $\boldsymbol{s_j} \in \mathcal{S}$.

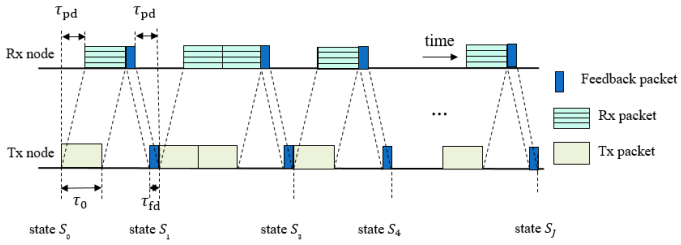

Fig. 1. An illustration of the delays involved in a typical packet exchange between the transmitter and the receiver node.

State transitions occur following a transition function Γ, based on information received via feedback. Finally, *agent* transits to the terminal state $\boldsymbol{s_J}$ (and thus $j = 0, \cdots, J$) to have all N bits transferred with totally K feedback packets sent out from Rx. The round-trip packet exchange duration includes the packet transmission duration τ_j, a two-way propagation delay $2\tau_{\text{pd}}$ and a feedback duration τ_{fd}, as illustrated in Fig. 1.

In state $\boldsymbol{s_j}$, given a modulation scheme $\boldsymbol{a}$ with uncoded data rate $d(\boldsymbol{a})$, BER estimation model $\zeta(\cdot)$ predicts the uncoded BER $\hat{\epsilon}(\boldsymbol{a})$:

$$\hat{\epsilon}(\boldsymbol{a}) = \zeta(\boldsymbol{a}; \boldsymbol{\theta_j}), \tag{1}$$

where $\boldsymbol{\theta_j}$ denotes the parameters of $\zeta(\cdot)$, which are adapted as the CSI is updated. Shannon's channel capacity [24] determines the code rate limit $\hat{\rho}(\boldsymbol{a})$ for error-free communication. With the use of a good forward error correction (FEC) technique, one can achieve robust communication at rates close to (but strictly less than):

$$\hat{\rho}(\boldsymbol{a}) = 1 - f(\hat{\epsilon}(\boldsymbol{a})), \tag{2}$$

where the entropy is computed as $f(x) = -x \log_2 x - (1 - x) \log_2 (1 - x)$. The transmitter adds redundant bits to the information, forming codewords, resulting in effective data rate:

$$\hat{D}(\boldsymbol{a}) \approx d(\boldsymbol{a}) \hat{\rho}(\boldsymbol{a}). \tag{3}$$

The agent then evaluates a scheme $\boldsymbol{a}$ on the basis of $\hat{D}(\boldsymbol{a})$ and selects the optimal scheme $\boldsymbol{a}^*$ using:

$$\boldsymbol{a}^* = \underset{\boldsymbol{a} \in \mathcal{A}}{\operatorname{argmax}} \hat{D}(\boldsymbol{a}). \tag{4}$$

We define a model $\mathcal{M}(\cdot)$ that helps us decide FRI h:

$$h = \mathcal{M}\left(\{N'_j, r_j\}; \boldsymbol{\omega_j}\right), \tag{5}$$

where $\boldsymbol{\omega_j}$ represents the trainable parameters of model $\mathcal{M}(\cdot)$. The model operates on two parameters: the immediate throughput r_j, computed using previous h packets, and the percentage of transmitted bits N'_j. The parameters N'_j, and r_j are good indicators of the quality of $\boldsymbol{a}^*$.

After gathering the feedback information, the state $\boldsymbol{s_j} \equiv \{\boldsymbol{\theta_j}, N'_j, r_j, \boldsymbol{\omega_j}\}$ transits to the state $\boldsymbol{s_{j+h}}$ using the state transition function $\Gamma(\cdot)$, i.e.,

$$\begin{aligned} \boldsymbol{s_{j+h}} &= \Gamma(\boldsymbol{s_j}, \boldsymbol{a}^*, h) \\ &= \{\boldsymbol{\theta_{j+h}}, N'_{j+h}, r_{j+h}, \boldsymbol{\omega_{j+h}}\}. \end{aligned} \tag{6}$$

In transmitting N bits, it takes J data packets and K feedback packets (both of which are unknown). We wish to minimize the total time to transmit all N bits:

$$\text{minimize} \sum_{i=0}^{J} \tau_i + K(\tau_{\text{fd}} + 2\tau_{\text{pd}}). \tag{7}$$

III. Adaptive Modulation and Coding

A. BER estimation model

We consider a modem that uses Orthogonal Frequency Division Multiplexing (OFDM) for communication, but allows several parameters to be tuned. There are two key parameters in OFDM: the cyclic prefix length n_{p} and the number of subcarriers n_{c}. Another important parameter is the bandwidth B occupied by the OFDM signal. Before a packet is transmitted, $n_{\text{c}}, n_{\text{p}}$ and B are selected to optimize for the performance. An AMC scheme $\boldsymbol{a}$ is therefore defined as a point in $(n_{\text{c}}, n_{\text{p}}, B)$ space. The uncoded data rate $d(\boldsymbol{a})$ is then:

$$d(\boldsymbol{a}) = \frac{mBn_{\text{c}}}{n_{\text{c}} + n_{\text{p}}}, \tag{8}$$

where m is the number of bits per PSK symbol on each subcarrier use for the underlying OFDM carrier modulation (e.g. $m = 1$ for BPSK and $m = 2$ for QPSK).

In [15], the channel delay spread τ_{ds}, channel coherence time τ_{c} and, bandwidth B, were utilized to define boundaries c_1, c_2 and c_3

$$n_{\text{c}} > 2\pi B \tau_{\text{ds}} = Bc_1, \tag{9}$$

$$n_{\text{p}} > B\tau_{\text{ds}} = Bc_2, \tag{10}$$

$$n_{\text{c}} + n_{\text{p}} < B\tau_{\text{c}} = Bc_3, \tag{11}$$

in the $(n_{\text{c}}, n_{\text{p}})$ plane. These boundaries divided the region into a relatively good region represented by blue shaded color and a bad region represented by red shaded color (see Fig. 2). Schemes inside the good region are more likely to achieve a higher packet success rate which is usually associated with a lower uncoded BER [25]. In line with [15], a sigmoid function

$$s(d) = \frac{1}{1 + e^{-b_i d}}, \quad i = 1, 2, 3, \tag{12}$$

is utilized to characterize the BER estimation model based on the relative position of the point $(n_{\text{c}}, n_{\text{p}})$ with respect to the three boundaries c_i, $i = 1, 2, 3$ (see Fig. 2). The slope of the three sigmoid functions is controlled by b_i, $i = 1, 2, 3$. Additionally, there is a relationship between the bandwidth B and the BER as a broader bandwidth is likely to contain more noise and thus might result in a higher BER [26]. Based on this, a simple parametric BER estimation model $\zeta(\boldsymbol{a}; \boldsymbol{\theta})$ to estimate uncoded BER $\hat{\epsilon}(\boldsymbol{a})$ is proposed as:

$$\zeta(\boldsymbol{a}; \boldsymbol{\theta}) = (b_4 B + c_4) s(-d_1) s(-d_2) s(d_3), \tag{13}$$

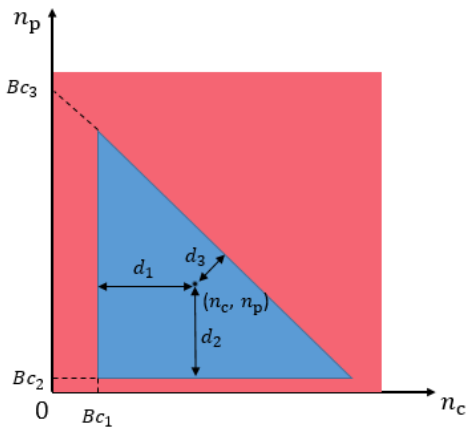

Fig. 2. Visualization of the boundaries c_1, c_2 and c_3 in the (n_c, n_p) plane.

$$d_1 = n_c - Bc_1, \tag{14}$$

$$d_2 = n_p - Bc_2, \tag{15}$$

$$d_3 = \frac{n_c + n_p - Bc_3}{\sqrt{2}}, \tag{16}$$

where d_1, d_2, d_3 are distances as shown in Fig. 2 and $\boldsymbol{\theta} \equiv (c_1, c_2, c_3, c_4, b_1, b_2, b_3, b_4)$.

B. Validation of BER estimation model

The BER estimation model presented in Section III-A is validated using experimental data that was collected in Singapore waters. Subnero M25M modems operating in the 18 to 32 kHz band were used for this data collection. The transmission range between the Tx and Rx was about 600 m, and the water depth was between 10 and 20 m. The BER for 1979 schemes $\boldsymbol{a} = (n_c, n_p, B)$ were measured, where n_c was set to different values from the set $\{64, 128, 256, 512, 1024, 2048\}$ and n_p ranged from 0 to 2046.

An ADAM optimizer [27] together with a maximal absolute error loss was utilized to train $\boldsymbol{\theta}$ on 70% of the data set. In Fig. 3, we compare the BER $\hat{\epsilon}$ estimated using the parametric model $\zeta(\cdot)$ with the actual BER ϵ measured for each (n_c, n_p, B) in the remaining 30% of the data set. Since the measured BER was observed to be similar between adjacent values of n_p, the result is only plotted for every n_c with n_p grouped with a bin size of 128. Furthermore, since the effect of B was observed to be small, all values of B for which the measurements were performed are clubbed together in the plot. We observe that the model $\zeta(\cdot)$ is able to approximate the median BER from sea measurements well.

C. Scheme selection policy

Since we have no knowledge of the quality of the communication link beforehand, the agent needs to make decisions on $\boldsymbol{a}$ while learning about the channel information via feedback. A well-known problem that occurs in scenarios like this is the trade-off between exploration and exploitation of different schemes. We need to select $\boldsymbol{a}$ given $\hat{\epsilon}(\boldsymbol{a})$ estimated using

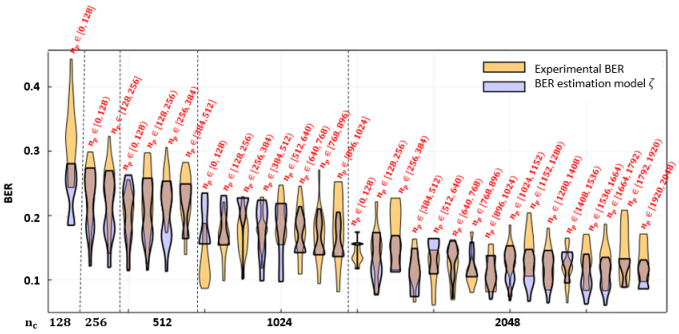

Fig. 3. Comparison of the measured BER in the field experiment and the estimated BER using model $\zeta(\cdot)$.

$\zeta(\boldsymbol{a}; \boldsymbol{\theta_j})$. Should we repeat decisions with lower $\hat{\epsilon}(\boldsymbol{a})$ (exploit) or select schemes that are never tried before hoping to gain greater rewards and expand the channel knowledge (explore)? The adaptive ε-greedy policy is a simple but efficient strategy to solve the explore-exploit dilemma and determines scheme $\boldsymbol{a}^*$ as following:

$$\boldsymbol{a}^* = \begin{cases} \underset{a \in \mathcal{A}}{\operatorname{argmax}} \Big(d(\boldsymbol{a}) \hat{\rho}(\boldsymbol{a}) \Big), & \text{with probability } 1 - \varepsilon \\ \text{Random}, & \text{with probability } \varepsilon \end{cases}, \tag{17}$$

where ε gradually decreases from 1 according to the common ratio ε_d along with the transmission of packets.

IV. Feedback Strategy

Gathering CSI via feedback from the receiver is essential for any AMC technique. However, due to the long propagation delays in underwater acoustic communications, waiting for feedback on every individual packet is expensive, and hence a policy to determine the FRI h that adapts with channel is necessary. A fixed FRI is commonly used in the literature while being able to adapt h to optimize for achieving higher throughput is an interesting problem. Conventional regression algorithms may help determine FRI h, but they require a large number of samples to train on. Such data with many different values of h is usually hard to obtain. A feedback strategy based on a heuristic sigmoidal function in [22] utilizes the immediate data rate of the previous FRI h to deduce the next h, and was demonstrated to achieve a significant reduction in the feedback overhead. We aim to improve on this heuristic and design a more generic adaptive feedback strategy next.

While in state $\boldsymbol{s_j}$, we receive the feedback and therefore update N'_j. The number of bits in each packet n_j and the packet duration τ_j remain unchanged in a particular transaction once an action $\boldsymbol{a}$ is selected. Therefore, the immediate throughput is computed using:

$$r_j = \frac{h n_j}{h\tau_j + 2\tau_{\text{pd}} + \tau_{\text{fd}}}. \tag{18}$$

Now that we know, r_j, N'_j and FRI, we are interested in determining h as a function of these. However such a function

is analytically unknown, and so we turn to ML to learn such a function. We build the model $\mathcal{M}(\cdot)$ using a simple 3-layer neural network (NN) with input being $\{r_j, N'_j, h\}$ and output as the predicted throughput $\tilde{r}_{j+h}$ and therefore,

$$h^* = \underset{h \in \mathcal{H}}{\operatorname{argmax}}\, \mathcal{M}\left(\{N'_j, r_j, h\}; \boldsymbol{\omega_j}\right), \tag{19}$$

where $\boldsymbol{\omega_j}$ contains the parameters of $\mathcal{M}(\cdot)$. The ADAM optimizer was used for training of $\boldsymbol{\omega_j}$ to minimize the MSE loss between the actual r_{j+h} and predicted $\tilde{r}_{j+h}$.

Since the action space $[\mathcal{A} \times \mathcal{H}]$ is large, collecting samples, i.e., $\{r_j, N'_j, h\} \rightarrow r_{j+h}$, for training $\mathcal{M}(\cdot)$ in real time is infeasible. We, therefore, propose a method to generate training samples through simulation, and to pre-train an initial estimate of parameter vector $\boldsymbol{\omega_0}$ (see Algorithm 1). We assume $\bar{\boldsymbol{\theta}}$ and thus $\zeta(\boldsymbol{a}; \bar{\boldsymbol{\theta}})$ represent specific ocean environments. To simulate the uncertainty in the environment, we generate random errors in a packet containing n bits following a Poisson distribution P, and thus the BER of scheme $\boldsymbol{a}$ is $\epsilon(\boldsymbol{a}) = \frac{P(\zeta(\boldsymbol{a}; \bar{\boldsymbol{\theta}})n)}{n}$. With different values of $\bar{\boldsymbol{\theta}}$, we collect training samples by simulating transmission with scheme $\boldsymbol{a}$ and h. To generate different values of $\bar{\boldsymbol{\theta}}$, we take inspiration from measured values of τ_{ds} and τ_{c} in different ocean [28]–[31], and randomly generate τ_{ds} less than 10 ms and τ_{c} between 0.01s and 2s and compute c_1, c_2, c_3. Without obvious quantitative relationship between the remaining parameters of $\bar{\boldsymbol{\theta}}$ and BER, b_4 and c_4 are uniformly generated from 0 to 1. Slopes b_1, b_2, b_3 are also uniformly generated between 0 and 1.

Algorithm 1 Algorithm to obtain an initial parameter estimates $\boldsymbol{\omega_0}$

Input: $[\mathcal{A} \times \mathcal{H}]$, transmission distance l, BER estimation model $\zeta(\cdot)$, and h selection model $\mathcal{M}(\cdot)$, ε_{d}.

1: Initialize state $\boldsymbol{s_0} = \{\boldsymbol{\theta_0}, N'_0 = 0, r_0 = 0, \boldsymbol{\omega_0}\}$ where $\boldsymbol{\theta_0}$ and $\boldsymbol{\omega_0}$ are randomized.
2: Generate $\bar{\boldsymbol{\theta}}$.
3: **while** $N'_j < 1$ **do**
4: Select $\boldsymbol{a}$ using (17) and randomly select $h \in \mathcal{H}$.
5: Transmit packets and receive feedback.
6: Perform state transition $\boldsymbol{s_j} \rightarrow \boldsymbol{s_{j+h}}$:
7: Update $\boldsymbol{\theta_j}$ based on $\boldsymbol{a}$ and ϵ from $\zeta(\boldsymbol{a}; \bar{\boldsymbol{\theta}})$.
8: Update $\boldsymbol{\omega_j}$ based on $\{r_j, N'_j, h\} \rightarrow r_{j+h}$.
9: Update N'_{j+h} and r_{j+h}.
10: **end while**
11: Reset initial state $\boldsymbol{s_0} = \{\boldsymbol{\theta_0}, N'_0 = 0, r_0 = 0, \boldsymbol{\omega_0}\}$ where $\boldsymbol{\theta_0}$ is randomized while the final $\boldsymbol{\omega_J}$ during the previous simulation is assigned to $\boldsymbol{\omega_0}$.
12: Back to line 2 until training ends.

Output: $\boldsymbol{\omega_0}$.

V. Simulation Results

We compare the proposed feedback strategy of adaptive model $\mathcal{M}(\cdot)$ with the pre-trained $\boldsymbol{\omega_0}$ with a *Random* strategy, where h is randomly picked between 1 and 50, and a *Regular* strategy where $h = 5, 10, 15, \cdots, 50$ is fixed a priori. Transmission distance l is set to 3 km and $\tau_{\text{fd}} = 100$ ms. m is set to 1 in (8) and $\varepsilon_{\text{d}} = 0.9$ in the adaptive ε-greedy policy. The simulation stops when $N = 100,000$ bits are transferred. The number of sub-carriers are set to $n_{\text{c}} = 64, 128, 256, 512, 1024, 2048$, and n_{p} ranges from 0 to 2048. 100 different $\bar{\boldsymbol{\theta}}$ values are generated to obtain a pre-trained $\boldsymbol{\omega_0}$. For different feedback strategies, policy Π is executed 100 times, and the average throughput computed is shown in Fig. 4. We observe that the policy Π when using *Random* strategy provides a throughput that is significantly poorer than what can be achieved via the proposed adaptive strategy. When using the *Regular* strategy, the median throughput initially increases with h, but gradually reduces when the value of h increases beyond a point. Selecting the optimal h a priori is generally difficult, but our proposed adaptive policy is able to select it dynamically.

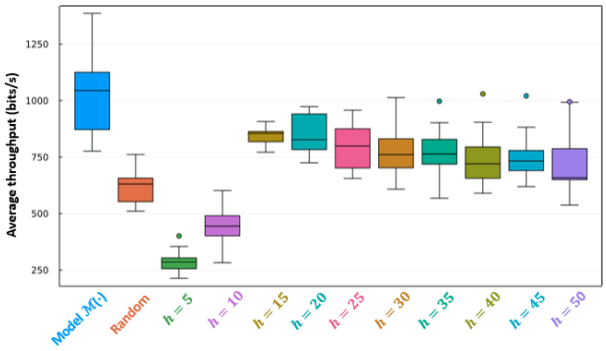

Fig. 4. Average throughput on a point-to-point link when using different feedback strategies.

VI. Conclusions

We evaluated the joint effect of AMC and the feedback strategy on the average throughput on a communication link. With the assistance of channel physics, our proposed BER estimation model for AMC achieves satisfactory channel performance with low computational complexity. An adaptive feedback strategy proved to be essential in deciding the appropriate times at which the feedback needs to be sent out.

References

[1] A. Radosevic, R. Ahmed, T. M. Duman, J. G. Proakis, and M. Stojanovic, "Adaptive ofdm modulation for underwater acoustic communications: Design considerations and experimental results," *IEEE Journal of Oceanic Engineering*, vol. 39, no. 2, pp. 357–370, 2014.

[2] L. Wan, H. Zhou, X. Xu, Y. Huang, S. Zhou, Z. Shi, and J.-H. Cui, "Adaptive modulation and coding for underwater acoustic ofdm," *IEEE Journal of Oceanic Engineering*, vol. 40, no. 2, pp. 327–336, 2015.

[3] A. Radosevic, R. Ahmed, T. M. Duman, J. G. Proakis, and M. Stojanovic, "Adaptive ofdm modulation for underwater acoustic communications: Design considerations and experimental results," *IEEE journal of oceanic engineering*, vol. 39, no. 2, pp. 357–370, 2014.

[4] P. Xia, S. Zhou, and G. Giannakis, "Adaptive mimo-ofdm based on partial channel state information," *IEEE Transactions on Signal Processing*, vol. 52, no. 1, pp. 202–213, 2004.

[5] D. Love and R. Heath, "Limited feedback power loading for ofdm," in *IEEE MILCOM 2004. Military Communications Conference, 2004.*, vol. 1, 2004, pp. 71–77 Vol. 1.

[6] A. Radosevic, R. Ahmed, T. M. Duman, J. G. Proakis, and M. Stojanovic, "Adaptive ofdm modulation for underwater acoustic communications: Design considerations and experimental results," *IEEE journal of oceanic engineering*, vol. 39, no. 2, pp. 357–370, 2014.

[7] L. Liu, L. Cai, L. Ma, and G. Qiao, "Channel state information prediction for adaptive underwater acoustic downlink ofdma system: Deep neural networks based approach," *IEEE Transactions on Vehicular Technology*, vol. 70, no. 9, pp. 9063–9076, 2021.

[8] R. Holzlöhner and C. R. Menyuk, "Use of multicanonical monte carlo simulations to obtain accurate bit error rates in optical communications systems," *Optics letters*, vol. 28, no. 20, pp. 1894–1896, 2003.

[9] B. Mazzeo and M. Rice, "On monte carlo simulation of the bit error rate," in *2011 IEEE International Conference on Communications (ICC)*, 2011, pp. 1–5.

[10] C. Fang, Q. Huang, F. Yang, X. Zeng, X. Li, and C. Gu, "Efficient bit error rate estimation for high-speed link by bayesian model fusion," in *Proceedings of the 2015 Design, Automation amp; Test in Europe Conference amp; Exhibition*, ser. DATE '15. San Jose, CA, USA: EDA Consortium, 2015, p. 1024–1029.

[11] C. Fang, F. Yang, X. Zeng, and X. Li, "Bmf-bd: Bayesian model fusion on bernoulli distribution for efficient yield estimation of integrated circuits," in *Proceedings of the 51st Annual Design Automation Conference*, ser. DAC '14. New York, NY, USA: Association for Computing Machinery, 2014, p. 1–6. [Online]. Available: https://doi-org.libproxy1.nus.edu.sg/10.1145/2593069.2593099

[12] A. A. Mohammed, L. Yu, M. Al-Kali, and E. E. B. Adam, "Ber analysis and evaluated for different channel models in wireless cooperation networks based ofdm system," in *2014 Fourth International Conference on Communication Systems and Network Technologies*, 2014, pp. 326–330.

[13] M. Neema, E. Gopi1, V. Reddy, and G. Mukesh, "Estimation of maximum achievable datarate and ber in spatial modulation scheme using artificial neural network based regression model," 04 April 2022.

[14] E. Lucas and Z. Wang, "Performance prediction of underwater acoustic communications based on channel impulse responses," *Applied Sciences*, vol. 12, no. 3, 2022. [Online]. Available: https://www.mdpi.com/2076-3417/12/3/1086

[15] P. Anjangi and M. Chitre, "Model-based data-driven learning algorithm for tuning an underwater acoustic link," in *2018 Fourth Underwater Communications and Networking Conference (UComms)*, 2018, pp. 1–5.

[16] Q. Liu, S. Zhou, and G. Giannakis, "Queuing with adaptive modulation and coding over wireless links: cross-layer analysis and design," *IEEE Transactions on Wireless Communications*, vol. 4, no. 3, pp. 1142–1153, 2005.

[17] M. Chitre, M. Motani, and S. Shahabudeen, "Throughput of networks with large propagation delays," *IEEE Journal of Oceanic Engineering*, vol. 37, no. 4, pp. 645–658, 2012.

[18] P. Mukherjee and S. De, "Dynamic feedback-based adaptive modulation for energy-efficient communication," *IEEE Communications Letters*, vol. 23, no. 5, pp. 946–949, 2019.

[19] ——, "cdip: Channel-aware dynamic window protocol for energy-efficient iot communications," *IEEE Internet of Things Journal*, vol. 5, no. 6, pp. 4474–4485, 2018.

[20] K. Mamat and W. Santipach, "On optimizing feedback interval for temporally correlated mimo channels with transmit beamforming and finite-rate feedback," *IEEE Transactions on Communications*, vol. 66, no. 8, pp. 3407–3419, 2018.

[21] S. Hong, S. Jo, and J. So, "Machine learning-based adaptive csi feedback interval," *ICT Express*, 2021. [Online]. Available: https://www.sciencedirect.com/science/article/pii/S2405959521001545

[22] S. Wu, M. A. Chitre, and P. Anjangi, "Monte carlo tree search and delay-aware feedback adaptation for underwater acoustic link tuning," 2021.

[23] M. A. Chitre, J. R. Potter, and S. H. Ong, "Viterbi decoding of convolutional codes in symmetric ¡emphasis emphasistype="italic"¿¡/emphasis¿ -stable noise," *IEEE Transactions on Communications*, vol. 55, no. 12, pp. 2230–2233, 2007.

[24] C. E. Shannon, "A mathematical theory of communication," *The Bell System Technical Journal*, vol. 27, no. 3, pp. 379–423, 1948.

[25] G. Chen, E. Rodriguez-Villegas, and A. J. Casson, "Chapter 5.1 - wearable algorithms: An overview of a truly multi-disciplinary problem," in *Wearable Sensors*, E. Sazonov and M. R. Neuman, Eds. Oxford: Academic Press, 2014, pp. 353–382. [Online]. Available: https://www.sciencedirect.com/science/article/pii/B9780124186620000052

[26] K. Narayanan and J. Doherty, "A convex projections method for improved narrow-band interference rejection in direct-sequence spread-spectrum systems," *Communications, IEEE Transactions on*, vol. 45, pp. 772 – 774, 08 1997.

[27] D. P. Kingma and J. Ba, "Adam: A method for stochastic optimization," 2017.

[28] M.-S. Kim, T.-S. Lee, T.-H. Im, and H.-L. Ko, "The analysis of coherence bandwidth and coherence time for underwater channel environments using experimental data in the west sea, korea," in *OCEANS 2016 - Shanghai*, 2016, pp. 1–4.

[29] M. Chitre, J. Potter, and O. Heng, "Underwater acoustic channel characterisation for medium-range shallow water communications," in *Oceans '04 MTS/IEEE Techno-Ocean '04 (IEEE Cat. No.04CH37600)*, vol. 1, 2004, pp. 40–45 Vol.1.

[30] A. Malarkodi, G. Latha, and S. Srinivasan, "Characterization of underwater acoustic communication channel," 2020.

[31] S.-M. Kim, S.-H. Byun, S.-G. Kim, D.-J. Kim, S. Kim, and Y.-K. Lim, "Underwater acoustic channel characterization at 6khz and 12khz in a shallow water near jeju island," in *2013 OCEANS - San Diego*, 2013, pp. 1–4.